INSTITUTE OF PHYSICS PUBLISHING JOURNAL OF PHYSICS: CONDENSED MATTER

J. Phys.: Condens. Matter **18** (2006) 8195–8204 doi:10.1088/0953-8984/18/35/007

Direct observation of spectroscopic inhomogeneities on $La_{0.7}Sr_{0.3}MnO_3$ thin films by scanning tunnelling spectroscopy

R Di Capua[1,2], C A Perroni[1,4], V Cataudella[1,2], F Miletto Granozio[1], P Perna[1,3], M Salluzzo[1], U Scotti di Uccio[1,3] and R Vaglio[1,2]

[1] CNR-INFM/COHERENTIA, Italy
[2] Dipartimento di Scienze Fisiche, Università di Napoli, 'Federico II', Italy
[3] Di.M.S.A.T., Università di Cassino, Italy

E-mail: rdicapua@na.infn.it

Received 5 June 2006
Published 15 August 2006
Online at stacks.iop.org/JPhysCM/18/8195

Abstract

Scanning tunnelling spectroscopy measurements were performed on thin films of $La_{0.7}Sr_{0.3}MnO_3$ both at room temperature and liquid nitrogen temperature. While no inhomogeneities were recorded at liquid nitrogen temperature on any sample, clear evidence of spectroscopic inhomogeneities was evident in tunnelling conductance maps collected at room temperature. The investigated films exhibit a transition from a ferromagnetic-metallic to a paramagnetic-insulating state at around room temperature, so the observed spectroscopic features can be interpreted within a phase separation scenario. A quantitative analysis of the observed spectroscopic features is reported, pointing out the occurrence of phase modulation and its possible correlation with the properties of the system.

1. Introduction

The rich phase diagram and the colossal magnetoresistance [1] of manganites such as $La_{1-x}A_xMnO_3$ (where A is a divalent metallic atoms) strongly depend on the interplay between electron, spin, orbital and lattice degrees of freedom. It is widely accepted that, in many of these compounds for x close to $x = 0.3$, the observed transition from a ferromagnetic metallic (FM) to a paramagnetic insulating (PI) state is due to the double-exchange mechanism proposed by Zener [2] together with a strong Jahn–Teller coupling responsible for the polaronic character of carriers at high temperatures [3, 4]. Moreover, many studies pointed out the possible formation of phase separation (PS) between FM and PI nanoscopic domains near the Curie temperature (T_c) [5, 6]. While the existence of phase separation is supported by several theoretical approaches and experimental evidence [7–11], its characteristic length scale (nanoscopic versus

[4] Present address: IFF, Forschungszentrum Juelich, 52425 Juelich, Germany.

mesoscopic) and dependence on external perturbations are still widely debated. Some recent experiments have found indications that even multi-scale phase modulation phenomena can occur in manganites [12].

Besides the double-exchange mechanism and Jahn–Teller coupling, several studies have stressed the role of disorder in inducing the phase coexistence [13]; others proposed a metal–insulator transition induced by long-range elastic interactions that are known to be crucial in films [14–16] and bulk samples [17–19].

Within this framework, the scanning tunnelling microscope (STM) represents a powerful tool to investigate the inhomogeneous state. Scanning tunnelling spectroscopy (STS) performed by STM differs from most other techniques, since it allows us to image spectroscopic inhomogeneities, up to nanometre resolution, in real space. The direct observation of an inhomogeneous state in manganites near T_c through STS is therefore possible because of the different spectroscopic features of the paramagnetic and ferromagnetic phases: insulating- and metallic-like, respectively. Differential tunnelling conductance can be recorded as a function of position in the scanned area ($\mathrm{d}I/\mathrm{d}V$ maps), hence mapping the local density of states (LDOS) of the sample surface.

The presence of an inhomogeneous state has been observed clearly on $La_{1-x}Ca_xMnO_3$ (LCMO). STS unambiguously revealed the presence of inhomogeneous structures and patterns in LDOS close to $x = 0.3$, pointing out a submicrometre scale for inhomogeneities [8]. For what concerns $La_{1-x}Sr_xMnO_3$ (LSMO), the question is more controversial and puzzling. Although it has been suggested by some authors that the double-exchange mechanism could fully describe the behaviour of LSMO bulk [20, 21], results obtained with different techniques, such as resistivity data [22], optical conductivity [23], susceptibility measurements at low doping [24], photoemission and x-ray spectroscopy [25], provided indirect indications about the possible presence of an inhomogeneus state, even in bulk samples. STM measurements have not yet clarified the picture. To our knowledge, the only observation of electronic inhomogeneities on LSMO by STS was reported by Becker *et al* [26], but they mainly reported on a different relative abundance of conducting and insulating spots as a function of temperature, and there was no clear imaging of spatial features as for LCMO [8]. In contrast, Akiyama *et al* [27] observed magnetic domains on LSMO thin films with an LSMO-coated STM tip, but they measured homogeneous electronic LDOS with metallic tips.

In this paper, we report on directly imaged regions having, at room temperature, different spectroscopic signatures, by performing STS measurements on $La_{0.7}Sr_{0.3}MnO_3$ thin films. Considering the reproducibility of measurements, the electronic homogeneity systematically observed, in contrast, at liquid nitrogen temperature, and the absence of correlation between spectroscopy and topography, as discussed in the following, our results strongly suggest that a phase modulation can occur in LSMO when triggered by disorder and long-range strains.

In section 2 we briefly describe the film's fabrication and main characterization, as well as the experimental procedure adopted for the STS measurements. Section 3 reports the observed tunnelling results: $\mathrm{d}I/\mathrm{d}V$ maps on samples with different thicknesses at different temperatures, tunnelling spectra, STM topographies and basic comments on such results. Finally, in section 4 we perform a quantitative analysis and discuss our data and their interpretation.

2. Sample preparation and experimental details

$La_{0.7}Sr_{0.3}MnO_3$ thin films were fabricated by rf magnetron sputtering from a stoichiometric target on $SrTiO_3$ (STO) substrates with orientations (100) and (110). The deposition temperature was 840 °C, with a substrate-to-target distance of 40 mm and a sputtering pressure (50% O_2, 50% Ar) of 50–70 Pa; such conditions led, on both substrates, to a growth rate of

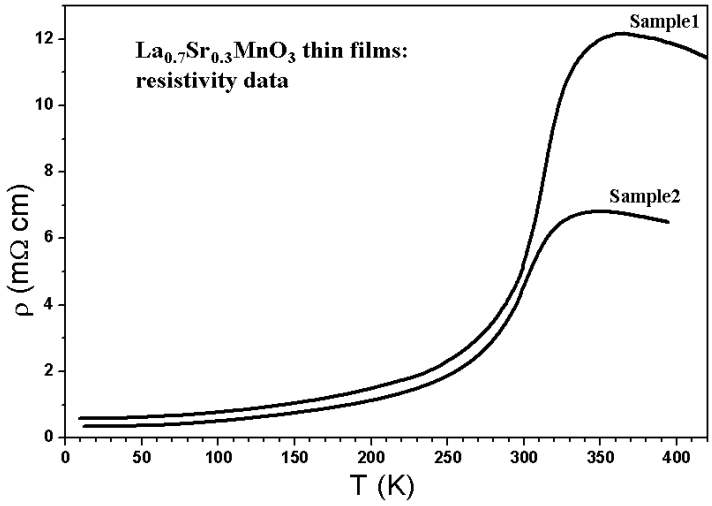

Figure 1. $\rho(T)$ curves for the investigated $La_{0.7}Sr_{0.3}MnO_3$ films. The transition temperature has been evaluated from these curves by taking the temperature of the maximum derivative [5].

Table 1. Main properties of reported $La_{0.7}Sr_{0.3}MnO_3$ films.

Name	Substrate	Thickness (nm)	T_p (K)	T_c (K)
Sample 1	STO(110)	40	350	310
Sample 2	STO(100)	10	350	300

0.3 Å s^{-1}. The films' stoichiometry was measured by energy dispersion spectroscopy (EDS) and Rutherford backscattering (RBS). Transport and magnetic characterizations are provided in more detail elsewhere [22, 28].

Figure 1 shows resistivity versus temperature ($\rho(T)$) curves. The plotted curves refer to the same films, grown on (STO) substrates (orientation given in table 1), for which STS measurements are reported. T_p represents the temperature of maximum resistivity; T_c values can be estimated from the maximum slope of $\rho(T)$ [5]. Table 1 summarizes the main properties of the films. We stress that, unlike bulk samples, LSMO films are characterized by a metal–insulator transition at $x = 0.3$.

STM experiments were performed in an inert helium atmosphere. The films were mounted on the STM scanner head and sealed in helium soon after the fabrication, limiting air exposure to preserve the surface quality. We used PtIr metallic tips, fabricated by an electrochemical etching procedure, which guarantees sharpness and reproducibility. The tips were tested by routinely achieving atomic resolution on graphite and $NbSe_2$ and flat conductance spectra on Au. In the experiments on LSMO films, the junction quality was checked, as in the report in [29], through the reproducibility of tunnel spectra versus tunnel resistance and of topographic details without artefacts. These checks were performed before and after any measurement run.

Topographic images were acquired in constant current mode, while tunnelling spectra (tunnelling current and differential conductance versus bias voltage curves) were recorded by disconnecting the feedback loop and using a standard lock-in technique. Tunnelling conductance maps were imaged through current image tunnelling spectroscopy (CITS) measurements. In this technique, the tip is moved from one point to another, on a scan line, with the current kept constant by the feedback loop, as in the topographic mode. However,

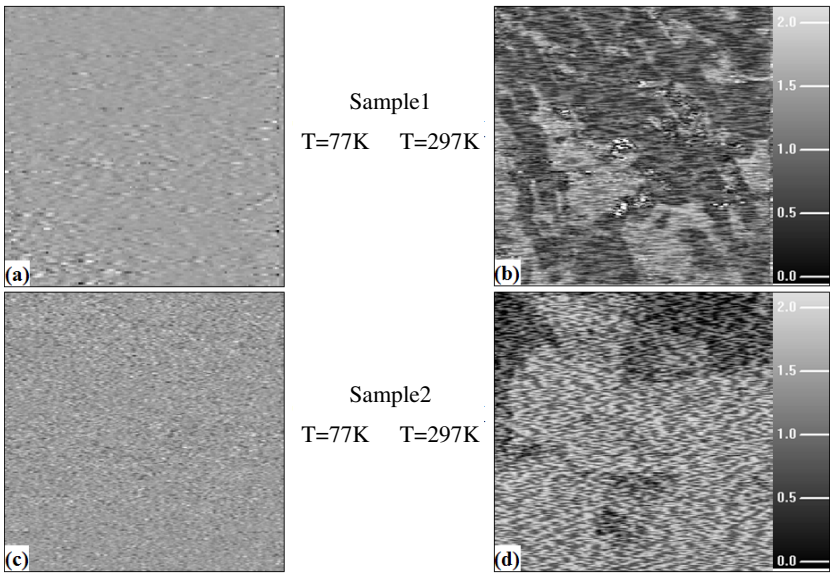

Figure 2. $\mathrm{d}I/\mathrm{d}V$ maps, 500 × 500 nm^2: (a) on sample 1 at $T = 77$ K and (b) at $T = 297$ K; (c) on sample 2 at $T = 77$ K and (d) at $T = 297$ K. The maps were acquired at a scan rate of 2.7 nm s^{-1}, tunnel current of 100 pA, and bias voltage (tip to sample) of 2 V. The tip-to-surface distance was frozen, stabilizing the feedback loop at a bias voltage of 3 V. In these maps, the lighter colours represent a more conducting character of the surface. In the reported colour bars, the tunnel conductance (arbitrary units) is displayed.

at each point, the feedback is disconnected in order to acquire the tunnelling conductance at a fixed bias voltage. Thus, a $\mathrm{d}I/\mathrm{d}V$ map represents an image of the surface LDOS (whose distance from the Fermi level is determined by the bias) at a fixed energy; such an image is a powerful way to detect possible spectroscopic and electronic inhomogeneities on the sample. Different $\mathrm{d}I/\mathrm{d}V$ maps on the same scan area were recorded to check the reproducibility of the imaged spectroscopic structures. The absence of artefacts was also tested by repeating the measurements at different scan rates. On the contrary, the same scan rate and the same experimental parameters were considered when the results on different samples had to be compared.

The acquisition of typical spectroscopic maps required about 13 h to be completed. They were acquired both at room temperature and at 77 K. In the latter case, the thermal stability of the STM junction was guaranteed by the presence of liquid nitrogen. At room temperature, we experienced severe problems in achieving the stability required for such long STM operation. For this reason, to avoid distortions in the tunnelling conductance maps, only when the STM topographic scans showed reproducibility over a long time did we perform the spectroscopic measurements. Many days were often necessary before the $\mathrm{d}I/\mathrm{d}V$ map could be acquired.

3. Experimental results

Figure 2 summarizes the main observed features on sample 1 and sample 2. Tunnelling conductance maps are reported. In the maps, the lighter colour represents higher tunnelling conductance, i.e. a more metallic character of the surface. All $\mathrm{d}I/\mathrm{d}V$ maps were measured at a tip-to-sample bias voltage of 2 V, with a tunnel current of 100 pA. As already reported

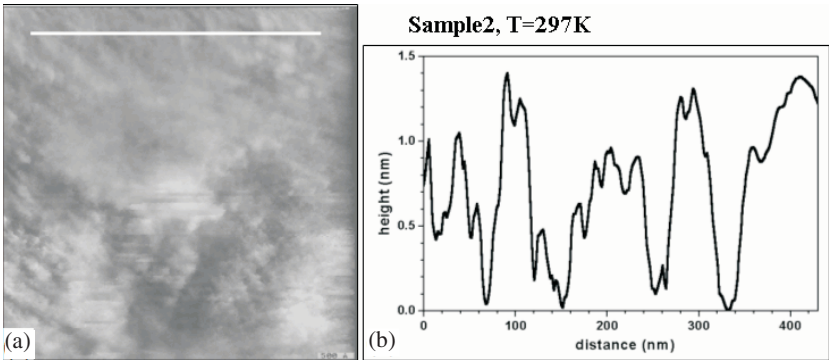

Figure 3. (a) STM topography on sample 2 at room temperature, on the same scanning area of the map in figure 2(d); (b) the height profile along the white line in the topography. The topography was recorded, simultaneously to the conductance map, at a tunnel current of 100 pA and a bias voltage of 3 V.

in other STS measurements [8], this relatively high tunnel resistance is needed because of the poor metallic properties of the surface of these compounds. The maps in figure 2 were acquired at a scan rate of about 2.7 nm s^{-1}.

At 77 K, well below T_c and therefore completely in the ferromagnetic state, dI/dV maps did not show evidence of inhomogeneities on any measured sample, exhibiting homogeneous LDOS over the whole imaged area (figures 2(a) and (c)). In contrast, maps at 297 K systematically showed submicrometre regions with sharply different spectroscopic features (figures 2(b) and (d)). From table 1, we see that the measurement temperature, 297 K, corresponds to a temperature slightly lower than T_c for both samples. This circumstance agrees with most PS theoretical works, which predict that separation effects are expected in the temperature range around the transition, where insulating (paramagnetic) clusters could appear even below the transition temperature. Furthermore, we note that the tunnelling dI/dV values recorded at 77 K correspond to the more conducting state in the 297 K maps, as discussed in the following.

Films with two different thicknesses, 40 and 10 nm, were measured.

From tunnelling conductance maps on 40 nm thick films, no differences were observed on samples grown on both STO(110) and STO(100). A dI/dV map acquired at room temperature on sample 1 is reported in figure 2(b). Figure 2(d) represents a dI/dV map at room temperature on sample 2, a 10 nm thick film on STO(100) (good quality films with this thickness were only obtained on this substrate).

The clear appearance of 'islands' in the LDOS at room temperature was found on every sample at room temperature. The relative abundance of conducting and insulating zones in each map depends on the imaged scanned area; however, the typical lateral size of the islands ranges on a submicrometre scale, being of the order of 100–300 nm (depending on the single island).

A comparison between spectroscopic and topographic features has been performed, in order to check if spectroscopic and topographic features show some degree of correlation. Figure 3(a) shows a topographic image on sample 2 on the same area of the dI/dV map (simultaneously acquired) reported in figure 2(d).

The data show a smooth surface: the height profile along the white line (crossing regions with different spectroscopic signatures), plotted in figure 3(b), presents a peak-to-peak roughness lower than 15 Å over a range of more than 4000 Å. Such a surface therefore

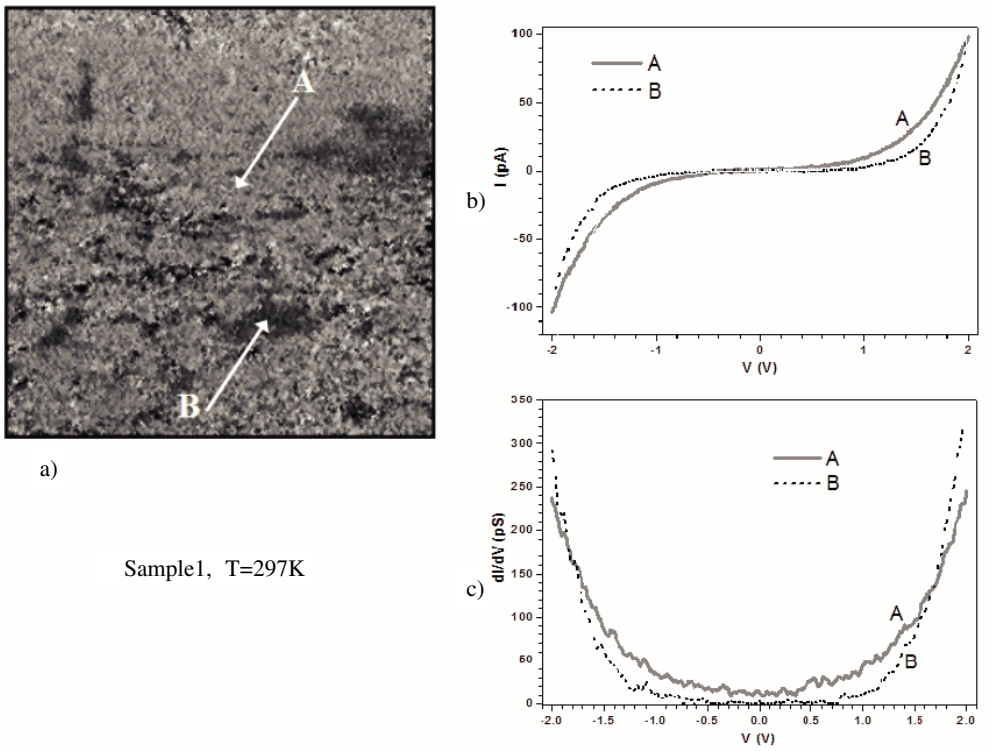

Figure 4. (a) $\mathrm{d}I/\mathrm{d}V$ maps, $500 \times 500\ \mathrm{nm}^2$, on sample 1 at $T = 297$ K; in the highlighted points A and B, tunnelling current and conductance versus bias voltage curves were acquired; the curves are reported in (b) (current) and (c) (conductance).

represents a good test to prove the absence of systematic correspondences between the two kinds of measurement. This claim can be supported quantitatively by evaluating the correlation coefficient of the two (spectroscopic and topographic) two-dimensional value distributions:

$$R = \frac{\sigma_{ct}^2}{\sqrt{\sigma_c^2 \sigma_t^2}} = \frac{ij\sum\left(\frac{C_{ij}-\overline{C}}{\overline{C}}\right)\left(\frac{T_{ij}-\overline{T}}{\overline{T}}\right)}{\sqrt{ij\sum\left(\frac{C_{ij}-\overline{C}}{\overline{C}}\right)^2 ij\sum\left(\frac{T_{ij}-\overline{T}}{\overline{T}}\right)^2}}. \tag{1}$$

In the above formula, C_{ij} and T_{ij} are the conductance and topography values respectively, measured at each pixel, while $\overline{C}$ and $\overline{T}$ are their average values; σ_{ct}^2, σ_c^2 and σ_t^2 are the covariance and the variances of the two distributions. The coefficient R ranges from -1 to 1, 1 and -1 representing the complete correlation and anticorrelation between the two data sets, respectively. For the measurements reported in figures 2(d) and 3(a), we calculated $R = 3 \times 10^{-2}$. It is worth noting that the topographic image used in this calculation was acquired simultaneously to the conductance map: during the CITS measurement, the height value was recorded at each pixel before disconnecting the feedback. As a consequence, we can exclude any thermal drift effect having produced displacements from one measure to another destroying a possible correlation.

In figure 4, two spectra, acquired with the tip well within an insulating and a conducting island respectively, are plotted. Both current and conductance curves reflect the different spectroscopic character of the two regions. The difference in the tunnelling spectra taken on

surface portions with different conductance is not extremely marked: this agrees with most of the reported tunnelling measurements on manganites. The conductance spectra show a gap-like DOS depletion around the Fermi level in both regions, but deeper and more pronounced in the insulating one. A rough estimation of the half-width of such a conduction gap gives values of about 1 and 0.6 V for the insulating and conducting islands, respectively.

The systematic observation of inhomogeneities just below T_c, the homogeneous appearance of all dI/dV maps at 77 K, the absence of correlation between dI/dV maps and topographic details, and the results in terms of tunnelling spectra, make us confident that the observed spectroscopic inhomogeneities are related to electronic and LDOS, intrinsic, spatial differences, and are not connected to any accidental chemical inhomogeneity occurrence [5, 12].

In addition, we should point out the presence, in the dI/dV maps, of a modulation in the tunnelling conductance on a smaller length scale (about 10–20 nm), more evident in sample 2. We do not yet have a clear explanation of this feature. This nanoscale pattern is present both in conducting and insulating submicrometre regions. At the moment, we are not able to check if this feature is intrinsic or if it is due to extrinsic effects. Some work in this direction is in progress.

We end this section by mentioning that we observed both dI/dV patterns also after thermal cycles, and they were reproducible (including the nanometre-scale modulation details) when changing the scan rate. This strongly suggests that the measured dI/dV features are not artefacts related to the tip–sample interaction.

4. Analysis and discussion

A more quantitative analysis can be developed. Figure 5 reports the dI/dV profile along scan lines in the maps recorded at room temperature on sample 1 and sample 2 (figures 5(a) and (c)), and the histogram distribution of the dI/dV values on the maps (figures 5(b) and (d)). All maps were recorded in the same conditions (described above), so a direct comparison between the values is possible. The histograms report, separately for conducting and insulating large islands, the relative counting frequency of the tunnel conductance values plotted in the dI/dV profiles. They represent a good synthesis of the information included in the maps and in the conductance line profiles. Indeed, the maps make evident the presence of inhomogeneities, but do not provide quantitative details on the tunnelling conductance values; on the other hand, the dI/dV line profiles allow an immediate comparison between spectroscopic measurements on different films and at different temperatures, but only on a very small portion of the experimental data. A histogram shows the quantitative content of a conductance profile, but representative of the entire area imaged in the map.

From the dI/dV profiles (figures 5(a) and (c)), the average values, taken on a line portion inside a 'single-colour' region of the map, put in evidence the LDOS separation. The highest dI/dV value, i.e. the one corresponding to the more conducting regions, is very close to the one recorded on the whole map at 77 K (ranging between 1.3 and 1.5 in the adopted units). The lowest one (corresponding to the more insulating regions) is reproduced well from one sample to another and from one (less conducting) island to another. The two average values look clearly distinguishable, from both the profile and the histograms, resembling the sharpness of features shown by the maps. The double-peaked feature, as well as the periodic-like modulation in the line profiles, are just a consequence of the above-mentioned nanometre-scale modulation in the dI/dV maps.

Several mechanisms have been proposed to explain the stabilization of submicrometre-scale domains with different electronic and magnetic properties [13–16].

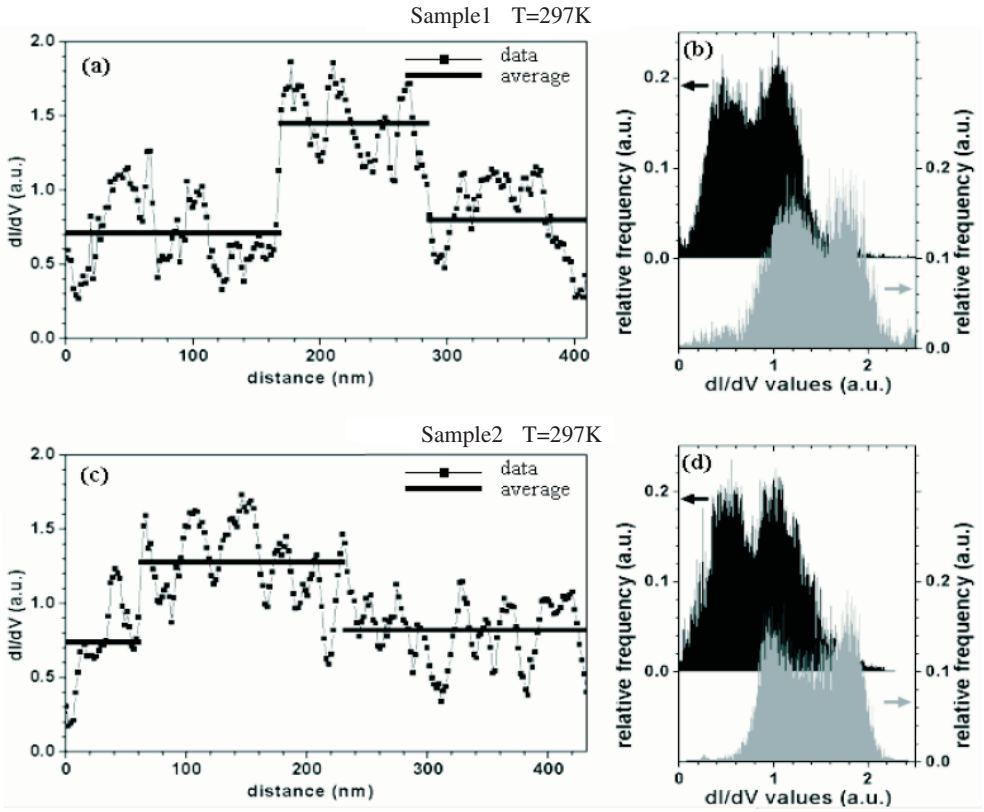

Figure 5. STS room temperature map analysis, concerning: (a) $\mathrm{d}I/\mathrm{d}V$ profile along a line for sample 1 (40 nm thick); (b) $\mathrm{d}I/\mathrm{d}V$ value distribution for sample 1; (c) $\mathrm{d}I/\mathrm{d}V$ profile along a line for sample 2 (10 nm thick); (d) $\mathrm{d}I/\mathrm{d}V$ value distribution for sample 2. Histograms have been plotted separately for the conducting and insulating large regions, and vertically shifted for clarity.

(This figure is in colour only in the electronic version)

However, while for the LCMO the coexistence of two phases around T_c, for x close to 0.3, is nowadays widely accepted, the existence of inhomogeneities between ferromagnetic metallic and paramagnetic insulating regions in LSMO at $x = 0.3$ is somehow unexpected. This is due to a more pronounced metallic character of LSMO than LCMO that obscures the formation, below T_c, of insulating clusters resembling the phase above the transition.

Our results, which clearly support the existence of submicrometre domains in LSMO films, can be understood if we remember two experimental observations. First of all, Mannella *et al* [25] have shown that LSMO single crystals exhibit different types of lattice distortions. These are smaller than in the LCMO case but, still, they could trigger a phase separation in LSMO. A second important observation is that, unlike single crystal, LSMO films at $x = 0.3$ exhibit an insulating-like decrease of $\rho(T)$ above T_p (see figure 1). These circumstances suggest that LSMO thin films can be considered, from this point of view, more similar to the LCMO system than to the LSMO single crystal. The difference between single crystal and films, in our opinion, can be interpreted in terms of the role played by disorder and strain in films. Actually, our observations are consistent with what has been reported by some of us in [22], where $\rho(T)$ curves for samples with different degrees of disorder were analysed using a model

based on the PS scenario. Such an analysis provided a good fit of the data for samples having the highest residual resistivity and the least metallic behaviour at high temperature; it should be remarked that those samples exhibited ρ_0 values very similar to those of sample 1 and sample 2 reported in figure 1. The same model resulted in a poor fitting of data for a sample with lower resistivity, i.e. with a more metallic character. This occurrence suggests that disorder can play an important role in films favouring a metal–insulating crossover and submicrometre phase coexistence, as proposed in [30]. It is worth noting that, alternatively to or in combination with disorder, the stress field induced by the substrate might play a major role in tuning the observed inhomogeneities [12]. In the case of LCMO films, the effect of stress has been studied and reported in [31].

Finally, concerning the lower average $\mathrm{d}I/\mathrm{d}V$ value observed in metallic regions of sample 2, it has the lowest T_c, and therefore it could be merely a consequence of the closest transition point. However, since the difference in the T_c s is very small and the transitions are quite broad, we cannot exclude an effect of the finite thickness [32] on this very thin film.

In conclusion, we have provided a clear, direct observation of inhomogeneities in the surface LDOS on $La_{0.7}Sr_{0.3}MnO_3$ thin films using STS spectroscopy close to T_c. The main experimental finding is represented by the coexistence, in films grown on STO(110) and STO(100), of two phases with different electronic features just below the transition temperature from the insulating-paramagnetic to the metallic-ferromagnetic state. The same measurements well below T_c show an homogenous aspect of the surface LDOS, which proves, as well as other circumstances discussed, that we observed intrinsic properties of the measured sample. Our data strongly suggest that the observed spectroscopic (electronic) pattern is related to the magnetic transition in the compound, which are in agreement with the phase separation scenario predicted for manganites and are still debated in the case of the LSMO system. The clearly observed islands on the sub-micrometre length scale, and in particular its apparent correlation with the disorder of the sample and with the substrate, seem to indicate the possibility of driving the phase separation by acting on strain and disorder. Concerning the observed conductance modulation on the smaller scale, although its presence in the recorded $\mathrm{d}I/\mathrm{d}V$ maps and in related analysis cannot be ignored, it requires a deeper investigation and measurements in order to clarify its presence and behaviour.

References

[1] Jin S, Tiefel T H, McCormack M, Fastnacht R A, Ramesh R and Chen L H 1997 *Science* **264** 413
[2] Zener C 1951 *Phys. Rev.* **82** 403
[3] Mills A J, Littlewood P B and Shraiman B I 1995 *Phys. Rev. Lett.* **74** 5144
[4] Salamon M B and Jaime M 2001 *Rev. Mod. Phys.* **73** 583
[5] Dagotto E 2003 *Nanoscale Phase Separation and Colossal Magnetoresistance* (Berlin: Springer)
[6] Mathur N and Littlewood P 2003 *Phys. Today* **56** 25
[7] Uehara M, Mori S, Chen C H and Cheong S-W 1999 *Nature* **399** 560
[8] Fath M, Freisem S, Menovsky A A, Tomioka Y, Aarts J and Mydosh J A 1999 *Science* **285** 1540
[9] Lu Q, Chen C-C and de Lozanne A 1997 *Science* **276** 2006
[10] Adams C P, Lynn J W, Mukovskii Y M, Arsenov A A and Shulyatev D A 2000 *Phys. Rev. Lett.* **85** 3954
[11] McGill S A, Miller R I, Torrens O N, Mamchik A, Chen I-W and Kikkawa J M 2004 *Phys. Rev. Lett.* **93** 47402
[12] Kim K H, Uehara M, Kiryukhin V and Cheong S-W 2002 *Colossal Magnetoresistive Manganites* ed T Chatterji (Dordrecht: Kluwer–Academic)
Kim K H, Uehara M, Kiryukhin V and Cheong S-W 2002 *Preprint* cond-mat/0212113
[13] Dagotto E, Hotta T and Moreo A 2001 *Phys. Rep.* **344** 1
[14] Konishi Y, Fang Z, Izumi M, Manako T, Kasai M, Kuwahara H, Kawasaki M, Terakura K and Tokura Y 1999 *J. Phys. Soc. Japan* **68** 3790
[15] Fang Z, Solovyev I V and Terakura K 2000 *Phys. Rev. Lett.* **84** 3169
[16] Ogimoto Y, Nakamura M, Takubo N, Tamaru H, Izumi M and Miyano K 2005 *Phys. Rev.* B **71** 060403

[17] Calderon M J, Millis A J and Ahn K H 2003 *Phys. Rev.* B **68** 100401
[18] Ahn K H, Lookman T and Bishop A R 2004 *Nature* **428** 401
[19] Sarma D D, Topwal D, Manju U, Krishnakumar S R, Bertolo M, La Rosa S, Cautero G, Koo T Y, Sharma P A, Cheong S W and Fujimori A 2004 *Phys. Rev. Lett.* **93** 97202
[20] Furukawa N 1999 *Physics of Manganites* ed T A Kaplan and S D Mahanti (New York: Plenum)
[21] Furukawa N 2000 *Colossal Magnetoresistive Oxides* ed Y Tokura (New York: Gordon and Breach)
[22] Mercone S, Perroni C A, Cataudella V, Adamo C, Angeloni M, Aruta C, De Filippis G, Miletto F, Oropallo A, Perna P, Petrov A Yu, Scotti di Uccio U and Maritato L 2005 *Phys. Rev.* B **71** 064415
[23] Hartinger C, Mayr F, Loidl A and Kopp T 2004 *Preprint* cond-mat/0404023
[24] Deisenhofer J, Braak D, Krug von Nidda H-A, Hemberger J, Eremina R M, Ivanshin V A, Balbashov A M, Loidl A, Kimura T and Tokura Y 2005 *Preprint* cond-mat/0501443
[25] Mannella N A, Rosenhahn A, Booth C H, Marchesini S, Mun B S, Yang S-H, Ibrahim K, Tomioka Y and Fadley C S 2004 *Phys. Rev. Lett.* **92** 166401
[26] Becker T, Streng C, Luo Y, Moshnyaga V, Damaschke B, Shannon N and Samwer K 2002 *Phys. Rev. Lett.* **89** 237203
[27] Akiyama R, Tanaka H, Matsumoto T and Kawai T 2001 *Appl. Phys. Lett.* **79** 4378
[28] Scotti di Uccio U, Davidson B, Di Capua R, Miletto Granozio F, Pepe G, Perna P, Ruotolo A and Salluzzo M 2006 *J. Alloys Compounds* at press
[29] Renner C and Fisher O 1995 *Phys. Rev.* B **51** 9208
[30] Burgy J, Moreo A and Dagotto E 2004 *Phys. Rev. Lett.* **92** 97202
[31] Biswas A, Rajeswari M, Srivastava R C, Venkatesan T, Greene R L, Lu Q, de Lozanne A L and Millis A J 2001 *Phys. Rev.* B **63** 184424
[32] Sun J Z, Abraham D W, Rao R A and Eom C B 1999 *Appl. Phys. Lett.* **74** 3017